SUPPLEMENT MATERIAL

ROLE OF DLL4 / NOTCH IN THE FORMATION AND WIRING OF THE LYMPHATIC NETWORK IN ZEBRAFISH

Geudens et al.

SUPPLEMENTAL METHODS

SCREENING METHODS FOR EVALUATION OF LYMPHATIC DEVELOPMENT AND FUNCTIONALITY

SCORING OF TD AND PL STRING FORMATION IN ZEBRAFISH: Live screening and quantification of thoracic duct (TD) formation was performed on anaesthetized *Fli1:eGFP*^{y1} embryos (a few drops of 4 mg/ml Tricaine (Sigma) stock solution in 5 ml embryo water) at 6 dpf when this vessel was completely developed in control embryos. DAPT treated fish (see below) were screened at 4 dpf, since screening at 6 dpf became impossible because fish became opaque due to loss of trunk circulation and edema and many fish died between 4 and 6 dpf. For screening, images were acquired using Zeiss AxioVision 4.6 software on a Leica DM RBE fluorescence stereomicroscope equipped with a Zeiss AxioCam MrC5 digital camera (Carl Zeiss, Munich, Germany; Leica Microsystems, Wetzlar, Germany). For reasons of standardization and to correct for slight differences in embryo size, the percentage of thoracic duct formation was quantified by scoring its percentile presence in 10 consecutive somite segments in the trunk after the junction of DA and PCV (i.e. somites 5-15, see Supplemental Figure III E). For screening of thoracic duct formation, only embryos with normal overall morphology and normal trunk circulation were included. All data are based on scorings of 33-185 embryos per condition, generated in at least 3 independent experiments. All analyses were performed by investigators blinded for the experimental treatment. Because the penetrance of the lymphatic phenotype was variable (see Supplemental Note II), we also determined the fraction of embryos with severe, intermediate or subtle lymphatic defects for each

treatment dose. Since parachordal lymphangiobast (PL) cells develop initially from lymphangiogenic secondary sprouts in a segmented pattern (Supplemental Figure I),[1] screening of PL string formation in the 10-somite segment of the trunk was performed in a similar manner at 52 hpf. Confocal imaging of *Fli1:eGFP^{y1}* embryos was performed using a Zeiss laser scanning microscope LSM510 or Leica SP2, SPE and SP5 confocal microscopes. Embryos were anaesthetized and positioned on a coverslip in a drop of 0.5% low melting point agarose. Fluorescence signal of *Stab1:YFP* images was transformed to a gray-scale image for better contrast.

FUNCTIONAL ASSESSMENT OF THE THORACIC DUCT: For functional studies, anesthetized larvae were subcutaneously injected with 1 nl fluorescent dextran (2.5 mg/ml) into the muscle mass of the posterior trunk by using glass capillaries and a conventional microinjection setup.[2]

IN VIVO "LEC-LABELING" AND FACS SORTING OF LABELED LECS: LEC labeling was performed on anaesthetized (a few drops of 4 mg/ml Tricaine (Sigma) stock solution in 5 ml embryo water) *Fli1:eGFP^{y1}* zebrafish larvae of 4 weeks old. Tetramethyl-rhodamine-dextran (TRITC-dextran; molecular weight 2000 kDa) was injected intramuscularly into the tail somites. After 3-4 days the dye had been drained by the lymphatics and was taken up by the LECs through pinocytosis. To obtain single cell supspensions, tails of at least 10 LEC labeled fish were collected, washed with distilled water, chopped, and incubated in 0.25% trypsin at 28°C until almost completely digested. The reaction was stopped by addition of 100μl FCS to inhibit the trypsin and the cell suspension was loaded on top of a Cell strainer tube with blue filter cap (40μm; BD Biosciences) for filtration. After pelleting of the cells (5min, 200g), the cell suspension was washed with 1ml dPBS containing 2% FCS, and viable cells were counted using trypan blue exclusion. After pelleting the cells were resuspended at a concentration of 10^6 cells/ml in FACS buffer (dPBS containing 1% FCS, filtered). Cells were sorted using a FACSAria (Becton Dickinson), taking care to exclude possible doublets or cell clusters. Non-injected GFP$^+$ *Fli1:GFP^{y1}* and TRITC-dextran injected GFP$^-$ embryos were used as controls for proper compensation and gate setting. On average 25000 GFP$^+$TRITC$^+$ LECs and 50000 GFP$^+$TRITC$^-$ BECs were sorted directly in lysis buffer (RLT containing 1% β-

mercaptoethanol) and processed for RNA extraction using the RNeasy kit (qiagen).

TIME LAPSE IMAGING: Embryos were mounted in 0.5% low melting point agarose in a culture dish with a cover slip replacing the bottom. Imaging was performed with a Leica SP2 or SP5 confocal microscope using a 10x, 20x or 40x objective with digital zoom. Timelapse analysis was compiled using ImageJ software (http://rsb.info.nih.gov/ij/). Time points were recorded every 10 minutes for the stated time period. A heated stage maintained the embryos at approximately 28.3 °C.

WHOLE-MOUNT IN SITU HYBRIDIZATION: Antisense probes specific for zebrafish *EphrinB2a,*[3] *Vegfr3,*[4] *Notch-1b, Notch-6, Dll4, Tie2, Dab2,*[1, 5] *Tbx20,*[6] *Cmlc2* or *MyoD* were used for whole-mount *in situ* hybridization of 28-48hpf embryos as described.[7] Stained embryos were paraffin- or plastic-embedded, sectioned and counterstained with nuclear fast red. In all figure panels the head of the embryo faces left and dorsal is up, unless stated otherwise.

QUANTITATIVE RT-PCR EXPRESSION ANALYSIS: RNA from FACS sorted LECs was reverse transcribed using the SuperScriptIII kit from Ambion. RNA from whole embryos was obtained by lysing in Trizol reagent and extraction using the RNeasy MiniElute Cleanup kit (Qiagen) and cDNA was prepared using the Quantitect Reverse Transcription kit (Qiagen). cDNA was subjected to qRT-PCR using zebrafish gene-specific primers/probe sets (Table S2).

CELL CULTURE EXPERIMENTS

HUVEC cells (Lonza, Invitrogen, Merelbeke, Belgium) and HUVEC/COS co-cultures were grown in EGM2-MV medium (Lonza, Invitrogen) at 37°C. COS cells were grown in standard DMEM medium (Lonza, Invitrogen) supplemented with 10% FBS, 2 mM glutamin, 100 U/ml penicillin, and 0.1 mg/ml streptomycin (Lonza).

COCULTURE ASSAY: COS cells stably expressing full length human Dll4 (COS^{Dll4}) or expressing GFP (COS^{CTR}) were prepared using the retroviral constructs LZRSpBMN-DLL4 and LZRSpBMN-WT, respectively.[8] HUVECs were co-seeded with COS^{Dll4} or COS^{CTR} cells in 6-wells at a density of 200,000 cells each, grown for 24 hours and harvested for RNA analysis by quantitative RT-PCR using human

gene-specific primers (Table S2). *PROLIFERATION ASSAY:* Primary LEC (HMVEC-DLy or HMVEC-LLy; Lonza, Invitrogen) were starved overnight in EGM2 medium (Lonza, Invitrogen) containing 0.1% serum and no growth factors (starvation medium). The starved cells were seeded at 2,000 cells per well in 96-well microtiter plates, after which proliferation was induced with fully supplemented EGM2-MV medium with or without increasing concentrations of DAPT (20-60 μM). Proliferation was measured as the number of viable cells after further culturing for 48 hours, expressed in % of DMSO control. Viable cells were quantified using the Rapid Cell Proliferation assay (Calbiochem, San Diego, CA).

SCRATCH WOUND MIGRATION ASSAY: Confluent monolayers of LECs growing in 0.1% gelatin-coated wells of a 24-well plate were starved overnight, pretreated in starvation medium containing 30 μM DAPT or 0.3% DMSO (control), scratch wounded and photographed (T0). The cells were further incubated for 24 hrs and photographed again (T24). Migration distance (gap width at T0 minus gap width at T24; 10 measurements per wound at regular intervals along the wound) was determined by image analysis using KS300 morphometry software, and is expressed relative to the control (DMSO).

TRANSWELL MIGRATION ASSAY IN CONDITIONS OF NOTCH INHIBITION: LECs were pretreated with DAPT (60 μM) or vehicle (DMSO) in starvation medium overnight, seeded at 30,000 cells per transwell on 0.1% gelatin-coated transwells in starvation medium with DAPT or DMSO, and cultured for 2 hours until adherence. Migration was induced by transferring the transwell insets into wells (bottom well) containing fully supplemented EGM2-MV medium with 100 ng recombinant human VEGF-C (Reliatech, TecoMedical NL, Nijkerk, the Netherlands), and DAPT or DMSO. Background migration was determined by including transwells with starvation medium in both the top and bottom well (baseline). After culturing for 16 hours, the non-migrated cells on the top side of the transwell filters were wiped off using PBS-soaked cotton swabs, and the transwells were fixed with 1% p-formaldehyde. The transwell filters were cut out and mounted upside-down on micrsocope slides with DAPI containing mounting medium. The filters were photographed under DAPI fluorescence at 20x magnification, and the nuclei were counted as a measure of

migrated cells. Five transwells were prepared per condition and five optical fields were counted and averaged per transwell filter.

TRANSWELL MIGRATION ASSAY IN CONDITIONS OF NOTCH ACTIVATION: LECs were starved overnight and seeded at 30,000 cells per transwell on transwell filters coated with BSA or with the extracellular domain of Dll4 (Dll4-ECD; R&D Systems Europe Ltd., Abingdon, UK) to activate the Notch pathway as described.[9] Further manipulation was as described above, using starvation medium in all top wells and fully supplemented medium containing VEGF-C in all bottom wells except for the baseline conditions. The filters were photographed under DAPI fluorescence at 10x magnification, Five transwells were prepared per condition and 1 central optical field was counted per transwell filter.

SUPPLEMENTAL NOTES

SUPPLEMENTAL NOTE I: LYMPHATIC DEVELOPMENT IN ZEBRAFISH EMBRYOS

In zebrafish embryos, the thoracic duct (TD) develops between the dorsal aorta (DA) and posterior cardinal vein (PCV); it is considered to be the first perfused lymphatic, as it drains interstitial dyes and has structural characteristics closely resembling mammalian lymphatics.[2, 10, 11] For reasons of clarity, formation of this early lymphatic network is schematically illustrated in Supplemental Figure I. Around 30 hpf, half of the secondary sprouts from the PCV, on average one per two unilateral somite segments, migrate radially in the ventral-dorsal direction to the horizontal myoseptum; these sprouts exist transiently (Supplemental Figure I A,A',B,B').[1, 12] At the horizontal myoseptum, cells of these sprouts then migrate tangentially in the anterior-posterior direction to form a string of parachordal lymphangioblasts (PL), which act as progenitors of future LECs in the TD (36 to 60 hpf); the PL string also exists only transiently. Since the secondary sprouts from the PCV, which give rise to the PL, participate in the process that leads to the formation of the TD, they have been termed "lymphangiogenic secondary sprouts". Indeed, the lymphangiogenic sprouts and PL cells give rise only to lymphatics but not to blood vessels, are not labeled in the arterial/venous *kdr-l:mCherryRed* marker line,[1] and fail to form upon silencing of genes that regulate lymphangiogenesis in mice and humans, e.g., *Ccbe1,*[1, 13] *Vegf-c,*[1] *Vegfr-3*[14] and *Synectin* (unpublished). The other secondary sprouts connect to the primary intersomitic vessels (ISVs), which thereby become intersomitic veins (vISV), and have therefore been termed "angiogenic secondary sprouts" (Supplemental Figure I A,B).[1, 12]

From 60 hpf onwards, the PL cells switch to radial migration again, and navigate both ventrally and dorsally alongside arterial intersomitic vessels (aISVs), whereby they form structures, that later persist as lymphatic intersomitic vessels (LISVs) (Supplemental Figure I C,D).[1] These radially migrating cells are termed LISV-PLs to distinguish them from the cells in the PL string. Once ventrally migrating LISV-PLs

reach their final location in-between the DA and PCV, they switch again to tangential migration, grow towards each other and fuse to establish the TD (3 to 6 dpf) (Supplemental Figure I D,D').[1, 2, 11, 12] While lymphangiogenic secondary sprouts migrate at a distance from and independently of aISVs, LISVs always navigated alongside aISVs, almost "creeping" over them in their initial dorsal and ventral trajectory, but never track alongside vISVs (Supplemental Figure I A',B',D'). This close association of LISVs with aISVs raised the question whether aISVs act as guidance templates for navigating LISVs-PLs.

SUPPLEMENTAL NOTE II: SILENCING STRATEGIES TO STUDY THE ROLE OF NOTCH IN LYMPH VESSEL FORMATION

SILENCING STRATEGIES: To explore a role for Notch signaling in lymphatic development, we made use of morpholino antisense oligonucleotides to silence every known zebrafish orthologue of the Notch ligands (DeltaA-D, Dll4, Jagged-1a/b, Jagged-2) and receptors (Notch-1a/b, -5, -6) as well as of the Notch activating presenilins (PS-1 and PS-2). For reasons of consistency, we used the zebrafish nomenclature: zebrafish Notch-5 and -6 are mammalian homologues of Notch-3 and -2, respectively, while zebrafish Notch-1a and -1b are duplicated mammalian orthologues of Notch-1.[15] Alternatively, Notch receptor activation was inhibited by exposing dechorionated 24-hpf embryos to *N*-[N-(3,5-difluorophenacetyl)-L-alanyl]-S-phenylglycine t-butyl ester (DAPT), a well known γ-secretase inhibitor (γ-secretase inhibitor IX; Calbiochem), that has been previously used to block Notch signaling in zebrafish embryos.[16]

SPECIFICITY OF THE PHENOTYPES: As Notch-family members have been implicated in angiogenesis,[17-19] we used submaximal doses of all morpholinos or of compound inhibitor to minimize secondary effects of vascular malformations on lymphatic development (referred to as "incomplete silencing" and "Notch hypomorphants"; Supplemental Figure II A-H and not shown). Furthermore, the compound inhibitor DAPT was added at later developmental stages, to avoid defects in early vascular development. We experimentally determined that treatment initiation at 43 hpf

induced lymphatic defects without inducing major vascular and developmental malformations. Treatment at earlier stages induced blood flow arrest, hemorrhages and edema in the majority of treated embryos. Only morphant embryos with a normal size, trunk circulation and blood flow, and without developmental delay, tissue malformations, general edema or toxic defects were included (Supplemental Figure III A-D; not shown). The lymphatic defects upon knockdown or compound treatment indeed were specific, as no overt changes in the formation and differentiation of the DA and PCV were noticeable (Supplemental Figure IV). Consistent with previous reports,[14, 20] some hyperbranching of the primary ISVs was detected in Dll4^{KD} hypomorphant embryos, but to a variable degree and in only 20% of Dll4^{KD} embryos (red arrowheads in Figure 1B; Supplemental Movie II). Also, no abnormalities in heart or somite development were observed (Supplemental Figure II I-L).

PHENOTYPE PENETRANCE: We speculate that the variably penetrant lymphatic phenotypes and spectrum of defects in the Notch hypomorphants is due to a combination of reasons, including the use of a submaximal dose of morpholino (incomplete silencing), technical limitations of injecting an identical dose of morpholino, genetic differences of the morphant embryos analyzed (outbred background; 10-fold variable RNA expression levels were observed for Dll4 between individual 4-dpf old embryos (copies Dll4/10^5 copies β-actin, median (range): 23.4 (6 – 58); *N*=24), uneven dispersion of morpholinos upon daughter cell division, and variable timing of venous/lymphatic secondary sprout formation along the PCV (occurring within a time window of 30 to 50 hpf [1]). As a result, achieving the necessary degree of silencing below the critical biological threshold at the distinct sprouting locations along the PCV becomes stochastic in such experimental conditions.

Phenotypic defects were dose-dependent, but for reasons of brevity, only the highest dose is shown. A standard control morpholino was used routinely and results were confirmed by using a second independent target-specific morpholino for silencing of Dll4, Notch-1b and PS-1.

SUPPLEMENTAL NOTE III: ACRONYMS FOR VASCULAR AND LYMPHATIC STRUCTURES IN THE ZEBRAFISH MODEL

aISV: arterial intersomitic vessel

BEC: blood endothelial cell

DA: dorsal aorta

DLAV: dorsal longitudinal anastomosing vessel

DLLV: dorsal longitudinal lymphatic vessel

ISV: intersomitic vessel

LEC: lymphatic endothelial cell

LISV: lymphatic intersomitic vessel

LISV-PL: parachordal lymphangioblasts that form the LISV

PAV: parachordal vessel

PCV: posterior cardinal vein

PL: parochordal lymphangioblast

TD: thoracic duct

vISV: venous intersomitic vessel

SUPPLEMENTAL FIGURES and MOVIES

SUPPLEMENTAL FIGURE I: MODEL OF LYMPHATIC DEVELOPMENT IN ZEBRAFISH EMBRYOS

In all panels, a schematic figure is shown on the left, and for panel A,B,D a high-magnification image of the blood and lymphatic vasculature at different stages of development in *Fli1:eGFP*^{y1} zebrafish on the right. For clarity, the confocal images are flanked by redrawings of the vessel contours. DA, dorsal aorta; DLAV, dorsal longitudinal anastomosing vessel; DLLV, dorsal longitudinal lymph vessel; ISV, intersomitic vessel; aISV, arterial ISV; LISV, lymphatic ISV; vISV, venous ISV; PCV, posterial cardinal vein; PL, parachordal lymphangioblast string; TD, thoracic duct. Permanent lymphatic structures (LISV, TD) are labeled dark green; transient lymphangiogenic structures (lymphangiogenic secondary sprouts; PL cells) are labeled light green. **A,A',** From around 30 hpf onwards, secondary sprouts arise from the PCV. About half of them will give rise to lymphatic structures and are therefore named lymphangiogenic secondary sprout (Ly sec. sprout; yellow arrows in A'). The other half of the secondary sprouts remain venous in nature (angiogenic secondary sprouts) (blue in A). **B,B',** By 48 hpf, the lymphangiogenic sprouts (yellow arrows in B') radially migrate dorsally to the level of the horizontal myoseptum, where they migrate tangentially to give rise to a transiently existing string of PL cells. The angiogenic sprouts connect to the aISV (red), which thereby will acquire a venous identity. **C,** Around 60 hpf, PL cells turn and switch from tangential to radial migration closely along aISVs, thereby forming lymphatic intersomitic vessels (LISVS); note the close association of LISVs with aISVs. LISVs that ascend form the dorsal longitudinal lymph vessel (DLLV), while those that descend form the TD. ISVs that connected to the angiogenic secondary sprouts progressively loose their arterial identity and acquire a venous fate. **D,D',** From 3 days onwards, the first TD fragments appear at distinct locations along the trunk and, via tangential migration, extend rostrally and caudally to merge into a complete TD. The LISV and TD are indicated by white arrows and arrowhead, respectively, in D'.

SUPPLEMENTAL FIGURE II: DEVELOPMENT OF EMBRYOS UPON INCOMPLETE INHIBITION OF DLL4

Complete silencing of Dll4/Notch signaling causes pronounced angiogenic defects.[17, 18, 21, 22] We therefore performed a detailed analysis, using high-resolution imaging, of the vasculature of control (A,C,E,G) and Dll4^{KD} hypomorphant *Fli1:eGFP^{y1}* embryos (10 ng Dll4^{SPL}; B,D,F,H). Scale bars: 100 μm. DA, dorsal aorta; PAV, parachordal vessel; PCV, posterior cardinal vein; TD, thoracic duct. **A,B,** The early vasculogenic stages proceeded normally in morphant embryos, resulting in the formation of properly sized and shaped axial vessels at timely developmental stages. Knockdown of Dll4 did not affect the timing or pathfinding of primary ISVs, or the subsequent formation of the DLAV (arrows) in embryos at 30 hpf. The DA is indicated by a red vertical bar, while the PCV is denoted by a blue vertical bar. **C,D,** Close-up images of the head vasculature at 30 hpf, showing similar appearance in control and Dll4^{KD} embryos. The arrow denotes the mid-cerebral vein. **E,F**, The subintestinal vessels (arrows) in 3-dpf Dll4^{KD} embryos displayed a largely comparable network morphogenesis with only minimal signs of hyperbranching. **G,H,** Image of a 12-dpf embryo, revealing that knockdown of Dll4 did not prevent the formation of the PAV, which develops only after the TD is established. Note the absence of the TD in the morphant embryo (asterisks in panel H), indicating that the TD defect persisted and was not rescued over time. The yellow arrowheads in G denote the course of the TD in the control embryo. The red arrowheads in H denote mild hyperbranching of the ISVs in the Dll4^{KD} embryo. **I-L,** Whole-mount *in situ* stainings for *Cmlc2* (I,J; 30 hpf) and *MyoD* (K,L; 48 hpf), showing that size and positioning of the heart (arrow) and somite development are normal in Dll4^{KD} embryos. Overall, at the morpholino concentrations used in our analyses, no overt angiogenic malformations were detected in Dll4^{KD} embryos prior to or during lymphangiogenesis. Further, imaging of the *Flt1:YFP* reporter line, in which only arterial ECs are labeled, confirmed that primary aISVs expressed the YFP transgene in Dll4^{KD} embryos, indicating that their initial arterial specification occurred normally (see Supplemental Movie II).

SUPPLEMENTAL FIGURE III: GENERAL MORPHOLOGY AND ANALYSIS OF TD FORMATION

A-D, Bright field images of 6-dpf control (A), Dll4^{KD} (10 ng Dll4^{SPL}; B), Notch-1b^{KD} (15 ng Notch-1b^{SPL}; C) and Notch-6^{KD} (15 ng Notch-6^{SPL}; D) embryos, showing normal overall morphological development. Only morphant embryos with a normal trunk circulation and body size, without developmental delay, tissue malformations, general edema or toxic defects were included in TD screening assays. **E,** TD quantification. DA, dorsal aorta; DLAV, dorsal longitudinal anastomosing vessels; ISV, intersomitic vessel; PCV, posterial cardinal vein; PL, parachordal lymphangioblast string; TD, thoracic duct. TD formation was quantified by measuring the length over which it formed in 10 consecutive somite segments (i.e. somites 5-15; demarcated by the green rectangle). Confocal images of control and morphant *Fli:eGFP^{y1}* embryos are depicted in the insets. Inset a: in the control embryo, a continuous TD formed over all 10 somite segments (100% TD formation; green arrowheads). Inset b: severely morphant embryo, in which the TD formed over only 10% (green arrowhead). Inset a' and b': schematic redrawing of the DA, TD and PCV in the embryo shown in inset a and b, respectively, with the TD or TD segment marked in green. Scale bars: 200 μm in A-D, 100 μm in E and insets of E.

SUPPLEMENTAL FIGURE IV: NORMAL ARTERIAL-VENOUS DIFFERENTIATION AFTER INHIBITION OF NOTCH.

A-R, Arterial-venous differentiation of the large axial vessels was evaluated upon incomplete silencing of the components of the Dll4/Notch signaling pathway that were shown in this study to affect lymphatic development. Therefore, whole-mount embryos were *in situ* stained for arterial (*EphrinB2a; Tbx20* [6, 23]) and venous (*Vegfr3; Dab2* [5, 24]) markers in control embryos (A-D) and in Dll4^{KD} (10 ng Dll4^{SPL}; E-H), Notch-1b^{KD} (15 ng Notch-1b^{SPL}; I-L), Notch-6 (15 ng Notch-6^{SPL}; M,N), PS-1 (15 ng PS-1^{ATG1}; O,P) or DAPT-treated (25 μM; Q,R) hypomorphant embryos. Staining was performed at 28 hpf (few hours prior to secondary sprout formation) for *EphrinB2a, Vegfr3 and Tbx20,* and at 48 hpf for *Dab2*, when arterial and venous differentiation of the DA and PCV were completed. Overall, expression of arterial markers in the DA and of venous markers in the PCV was comparable in control and morphant

embryos. Also, note that there is no ectopic expression of these markers. The DA is indicated by a red vertical bar, while the PCV is denoted by a blue vertical bar. DA, dorsal aorta; PCV, posterior cardinal vein. Scale bar, representative for all panels: 100 μm.

SUPPLEMENTAL FIGURE V: INHIBITION OF NOTCH DOES NOT AFFECT *IN VITRO* PROLIFERATION AND MIGRATION.

A, Primary LECs of dermal (HMVEC-DLy) and lung (HMVEC-LLy) origin were starved overnight, after which proliferation was induced with full growth medium with or without increasing concentrations of DAPT (30-60 μM). Proliferation was measured as the number of viable cells after further culturing for 48 hours, expressed in % of control. **B**, Migration of LECs, analyzed using a scratch wound healing assay, was not inhibited by DAPT (30 μM). **C**, Transwell migration of LECs in response to culture medium containing 10% FBS and 100 ng/ml VEGF-C in the lower compartment ("stimulated") was not affected by DAPT (60 μM). **D**, Transwell migration of LECs in response to culture medium containing 10% FBS and 100 ng/ml VEGF-C in the lower compartment was comparable, when cells were seeded on filters coated with BSA (control) or the extracellular domain of Dll4 (Dll4-ECD), previously shown to activate Notch signaling.[9] Error bars represent SEM; *N*=5-11.

SUPPLEMENTAL FIGURE VI: EXPRESSION OF NOTCH-1B.

Sagital section of an embryo at 30 hpf, when lymphangiogenic sprouting occurs, whole-mount stained for Notch-1b. DA, dorsal aorta; ISV, intersomitic vessel; PCV, posterior cardinal vein. Scale bar: 50 μm. Notch-1b is expressed in the DA and ISVs. A weak signal can be observed in the dorsal part of the PCV.

SUPPLEMENTAL MOVIE I: NORMAL FORMATION OF ARTERIAL AND VENOUS ISVS IN CONTROL EMBRYOS.

Confocal time-lapse video-imaging analysis of a control *Flt1:YFPxkdr-l:mCherryRed*

reporter embryo from 32 to 72 hpf (representative movie of >100 embryos analyzed), in which venous cells are red (CherryRed^{+}) and arterial cells yellow (YFP^{+}CherryRed^{+}). Imaging revealed normal progressive ventral-to-dorsal loss of the arterial YFP colour in approximately half of the ISVs, once connected by angiogenic secondary sprouts of the PCV. For instance, the second and third primary ISV (numbering according to the location at the start of the movie) retain their connection with the DA as well as their yellow arterial colour, and are thus arterial. In contrast, the fourth and fifth ISV loose their connection with the DA as well as their yellow arterial colour, progressively become red after establishing a connection with the PCV, and thus become venous ISVs.

Note: This *Flt1:YFP*x*kdr-l:mCherryRed* reporter does not label lymph vessels. However, since lymphangiogenic secondary sprouts emanate from the PCV (CherryRed^{+}) and the CherryRed protein is only degraded after some time, the presence of these lymphangiogenic secondary sprouts and of the PL cells is also transiently visible. For instance, around 40 hpf, red lymphangiogenic secondary sprouts can be seen adjacent to the second and third ISV. These secondary sprouts do, however, not connect to the primary ISVs, but migrate dorsally to the horizontal myoseptum, where they then migrate tangentially and form the PL string. The lymphangiogenic nature of the PL string is illustrated by the gradual loss of its residual mCherryRed colour beyond 52 hpf; this is not due to regression of the PL cells, since this string disappears only around 4 dpf, i.e. after giving rise to the LISVs (not visible in this reporter line) that descend ventrally to the level between the DA and PCV to form the TD. DA, dorsal aorta; PCV, posterior cardinal vein; PL, parachordal lymphangioblast string; TD, thoracic duct.

SUPPLEMENTAL MOVIE II: ARTERIAL-TO-VENOUS SHIFT OF ISVS IN DLL4^{KD} EMBRYOS

Confocal time-lapse video-imaging analysis of a Dll4^{KD} *Flt1:YFP*x*kdr-l:mCherryRed* embryo from 32-72 hpf (representative movie of >100 embryos analyzed), in which venous cells are red (CherryRed^{+}) and arterial cells yellow (YFP^{+}CherryRed^{+}). Imaging revealed progressive ventral-to-dorsal loss of the arterial YFP colour in all primary ISVs, when they became connected by an angiogenic secondary sprout and

therefore adopted a venous fate. In this embryo, there was a shift of lymphangiogenic to angiogenic secondary sprouting in all somites imaged.

SUPPLEMENTAL TABLE I: MORPHOLINO OLIGONUCLEOTIDE SEQUENCES

MO	MO sequence	Target	Ref
DeltaA^{ATG}	5'-CGCCGACTGATTCATTGGTGGAGAC-3'	Start site	
DeltaB^{ATG}	5'- CGCCATCTCGCTCACTTTATCCTAA-3'	Start site	
DeltaC^{ATG}	5'- GCACGTTAATAAAACACGAGCCATC-3'	Start site	
DeltaD^{ATG}	5'- AACAGCTATCATTAGTCGTCCCATG-3'	Start site	
Dll4^{ATG}	5'-GAGAAAGGTGAGCCAAGCTGCG-3'	Start site	
Dll4^{SPL}	5'-TAGGGTTTAGTCTTACCTTGGTCAC-3' 5'-TGATCTCTGATTGCTTACGTTCTTC -3'	Exon6/intron6 Exon4/intron4	20
Jag1a^{ATG}	5'-GTCTGTCTGTGTGTCTGTCGCTGTG-3'	5' UTR	
Jag1b^{ATG}	5'-CTGAACTCCGTCGCAGAATCATGCC-3'	Start site	
Jag2^{ATG}	5'-TCCTGATACAATTCCACATGCCGCC-3'	Start site	
Notch-1a^{ATG}	5'-TTCACCAAGAAACGGTTCATAACTC-3'	Start site	25, 26
Notch-1b^{ATG}	5'-ATGCATTCCTTCTTATGGATAGTCC-3'	Start site	
Notch-1b^{SPL}	5'-AATCTCAAACTGACCTCAAACCGAC-3'	intron28/exon29	20, 27
Notch-5^{ATG}	5'-ATATCCAAAGGCTGTAATTCCCCAT-3'	Start site	20, 28
Notch-6^{SPL}	5'-AGGTGAACACTTACTTCATGCCAAA-3'	exon7/intron7	20, 28
PS-1^{ATG1}	5'-CCGGGATCATAGAAACAGCGGGAAC-3'	5' UTR	
PS-1^{ATG2}	5'-CATTCTGCACTAAATCAGCCATCGG-3'	Start site	
PS-2^{ATG}	5'-CTCTTCACTGTCTGAGGTATTCATG-3'	Start site	29
control MO	5'-CCTCTTACCTCAGTTACAATTTATA-3'	Standard control MO (Gene Tools)	

For the previously unpublished morpholinos, silencing efficiencies of morpholinos directed against the ATG region were confirmed using a luciferase reporter assay, as previously described [30] (not shown).

SUPPLEMENTAL TABLE II: qRT-PCR PRIMER AND PROBE SEQUENCES

Zebrafish genes		
NOTCH1B	For Rev Probe	5'-AAC AAC CAA GAT CTT TCC CAT ATA CA-3' 5'-GCT CTA GCC ATT CGC ATT GAC-3' 5'-FAM-TTT GAT CCA TTG CCT CCA CGT CTC ACT-TAMRA-3'
DLL4	For Rev Probe	5'-CTT CAC CGG ACC CCT CTG T-3' 5'-TGG AAG CGG TCT TGA GTT TCT C-3' 5'-FAM-ATA CTA CGC CGT CAC AGC GCC CG-TAMRA-3'
β-ACTIN	For Rev Probe	5'-TGG TAT GGG ACA GAA AGA CAG CT-3' 5'-TTG GGT ACT TCA GGG TCA GGA-3' 5'-FAM-TCT TGC TCT GAG CCT CAT CAC CAA CG-TAMRA-3'
Human genes		
HES1	Hs00232622_m1 (Premade Taqman Gene expression assays, Applied Biosystems)	
HEY1	Hs00232618_m1 (Premade Taqman Gene expression assays, Applied Biosystems)	
HEY2	Hs00232622_m1 (Premade Taqman Gene expression assays, Applied Biosystems)	
NRARP	Hs01104102_s1 (Premade Taqman Gene expression assays, Applied Biosystems)	
VEGFR3	For Rev Probe	5'-TTC CTG GCT TCC CGA AAG T-3' 5'-AGG CCA AAG TCA CAG ATC TTC AC-3' 5'-FAM-ACC TGG CTG CTC GGA ACA TTC TGC-TAMRA-3'
PROX-1	For Rev Probe	5'-GTG CTT TGG CGA CGT CAT C-3' 5'-TCA GTG GAA CTG GCC ATC TG-3' 5'-FAM-TTC CGA ACC CCC TGG ACA CCT TTG-TAMRA-3'
LYVE-1	For Rev Probe	5'-CAA AGA TCC CAT ATT CAA CAC TCA A-3' 5'-GGG ATG CCA CCG AGT AGG TA-3' 5'-FAM-CTG CAA CAC AAA CAA CAG AAT TTA TTG TCA GTG ACA-TAMRA-3'
EPHRINB2	Hs00970627_m1 (Premade Taqman Gene expression assays, Applied Biosystems)	
SOX18	For Rev	5'-AGA ACC CGG ACC TGC ACA-3' (Sybr Green qRT-PCR) 5'-CAG CTC CTT CCA CGC TTT G-3'
COUP-TFII	Hs00819630_m1 (Premade Taqman Gene expression assays, Applied Biosystems)	
NEUROPILIN2	Hs00187290_m1 (Premade Taqman Gene expression assays, Applied Biosystems)	
CD31	For Rev	5'-TCT GCA CTG CAG GTA TTG ACA A-3' (Sybr Green qRT-PCR) 5'-CTG ATC GAT TCG CAA CGG A-3'
VE-CADHERIN	Hs00174344_m1 (Premade Taqman Gene expression assays, Applied Biosystems)	
ENDOGLIN	Hs00164438_m1 (Premade Taqman Gene expression assays, Applied Biosystems)	
β-ACTIN	Hs99999903_m1 (Premade Taqman Gene expression assays, Applied Biosystems)	
β-ACTIN	For Rev	5'-TGG CAC CAC ACC TTC TAC AAT G-3' (Sybr Green qRT-PCR) 5'-TAG CAA CGT ACA TGG CTG GG-3'

REFERENCES

1. Hogan BM, Bos FL, Bussmann J, Witte M, Chi NC, Duckers HJ, Schulte-Merker S. Ccbe1 is required for embryonic lymphangiogenesis and venous sprouting. *Nat Genet.* 2009;41:396-398.
2. Kuchler AM, Gjini E, Peterson-Maduro J, Cancilla B, Wolburg H, Schulte-Merker S. Development of the zebrafish lymphatic system requires VEGFC signaling. *Curr Biol.* 2006;16:1244-1248.
3. Chan J, Mably JD, Serluca FC, Chen JN, Goldstein NB, Thomas MC, Cleary JA, Brennan C, Fishman MC, Roberts TM. Morphogenesis of prechordal plate and notochord requires intact Eph/ephrin B signaling. *Dev Biol.* 2001;234:470-482.
4. Thompson MA, Ransom DG, Pratt SJ, MacLennan H, Kieran MW, Detrich HW, 3rd, Vail B, Huber TL, Paw B, Brownlie AJ, Oates AC, Fritz A, Gates MA, Amores A, Bahary N, Talbot WS, Her H, Beier DR, Postlethwait JH, Zon LI. The cloche and spadetail genes differentially affect hematopoiesis and vasculogenesis. *Dev Biol.* 1998;197:248-269.
5. Herpers R, van de Kamp E, Duckers HJ, Schulte-Merker S. Redundant roles for sox7 and sox18 in arteriovenous specification in zebrafish. *Circ Res.* 2008;102:12-15.
6. Szeto DP, Griffin KJ, Kimelman D. HrT is required for cardiovascular development in zebrafish. *Development.* 2002;129:5093-5101.
7. Chittenden TW, Claes F, Lanahan AA, Autiero M, Palac RT, Tkachenko EV, Elfenbein A, Ruiz de Almodovar C, Dedkov E, Tomanek R, Li W, Westmore M, Singh JP, Horowitz A, Mulligan-Kehoe MJ, Moodie KL, Zhuang ZW, Carmeliet P, Simons M. Selective regulation of arterial branching morphogenesis by synectin. *Dev Cell.* 2006;10:783-795.
8. Williams CK, Li JL, Murga M, Harris AL, Tosato G. Up-regulation of the Notch ligand Delta-like 4 inhibits VEGF-induced endothelial cell function. *Blood.* 2006;107:931-939.
9. Harrington LS, Sainson RC, Williams CK, Taylor JM, Shi W, Li JL, Harris AL. Regulation of multiple angiogenic pathways by Dll4 and Notch in human umbilical vein endothelial cells. *Microvasc Res.* 2008;75:144-154.
10. Jensen LD, Cao R, Hedlund EM, Soll I, Lundberg JO, Hauptmann G, Steffensen JF, Cao Y. Nitric oxide permits hypoxia-induced lymphatic perfusion by controlling arterial-lymphatic conduits in zebrafish and glass catfish. *Proc Natl Acad Sci U S A.* 2009.
11. Yaniv K, Isogai S, Castranova D, Dye L, Hitomi J, Weinstein BM. Live imaging of lymphatic development in the zebrafish. *Nat Med.* 2006;12:711-716.
12. Isogai S, Lawson ND, Torrealday S, Horiguchi M, Weinstein BM. Angiogenic network formation in the developing vertebrate trunk. *Development.* 2003;130:5281-5290.
13. Alders M, Hogan BM, Gjini E, Salehi F, Al-Gazali L, Hennekam EA, Holmberg EE, Mannens MMAM, Mulder MF, Offerhaus GJA, Prescott TE, Schroor EJ, Verheij JBGM, Witte M, Zwijnenburg PJ, Vikkula M, Schulte-Merker S, Hennekam RC. Mutations in *CCBE1* cause generalized lymph vessel dysplasia in humans. *Nat Gen.* 2009;41:1272-1274.
14. Hogan BM, Herpers R, Witte M, Helotera H, Alitalo K, Duckers HJ, Schulte-Merker S. Vegfc/Flt4 signalling is suppressed by Dll4 in developing zebrafish intersegmental arteries. *Development.* 2009;136:4001-4009.

15. Theodosiou A, Arhondakis S, Baumann M, Kossida S. Evolutionary scenarios of Notch proteins. *Mol Biol Evol.* 2009;26:1631-1640.
16. Geling A, Steiner H, Willem M, Bally-Cuif L, Haass C. A gamma-secretase inhibitor blocks Notch signaling in vivo and causes a severe neurogenic phenotype in zebrafish. *EMBO Rep.* 2002;3:688-694.
17. Hofmann JJ, Iruela-Arispe ML. Notch signaling in blood vessels: who is talking to whom about what? *Circ Res.* 2007;100:1556-1568.
18. Roca C, Adams RH. Regulation of vascular morphogenesis by Notch signaling. *Genes Dev.* 2007;21:2511-2524.
19. Sainson RC, Harris AL. Anti-Dll4 therapy: can we block tumour growth by increasing angiogenesis? *Trends Mol Med.* 2007;13:389-395.
20. Leslie JD, Ariza-McNaughton L, Bermange AL, McAdow R, Johnson SL, Lewis J. Endothelial signalling by the Notch ligand Delta-like 4 restricts angiogenesis. *Development.* 2007;134:839-844.
21. Phng LK, Gerhardt H. Angiogenesis: a team effort coordinated by notch. *Dev Cell.* 2009;16:196-208.
22. Swift MR, Weinstein BM. Arterial-venous specification during development. *Circ Res.* 2009;104:576-588.
23. Pendeville H, Winandy M, Manfroid I, Nivelles O, Motte P, Pasque V, Peers B, Struman I, Martial JA, Voz ML. Zebrafish Sox7 and Sox18 function together to control arterial-venous identity. *Dev Biol.* 2008;317:405-416.
24. Song HD, Sun XJ, Deng M, Zhang GW, Zhou Y, Wu XY, Sheng Y, Chen Y, Ruan Z, Jiang CL, Fan HY, Zon LI, Kanki JP, Liu TX, Look AT, Chen Z. Hematopoietic gene expression profile in zebrafish kidney marrow. *Proc Natl Acad Sci U S A.* 2004;101:16240-16245.
25. Holley SA, Julich D, Rauch GJ, Geisler R, Nusslein-Volhard C. her1 and the notch pathway function within the oscillator mechanism that regulates zebrafish somitogenesis. *Development.* 2002;129:1175-1183.
26. Riedel-Kruse IH, Muller C, Oates AC. Synchrony dynamics during initiation, failure, and rescue of the segmentation clock. *Science.* 2007;317:1911-1915.
27. Milan DJ, Giokas AC, Serluca FC, Peterson RT, MacRae CA. Notch1b and neuregulin are required for specification of central cardiac conduction tissue. *Development.* 2006;133:1125-1132.
28. Lorent K, Yeo SY, Oda T, Chandrasekharappa S, Chitnis A, Matthews RP, Pack M. Inhibition of Jagged-mediated Notch signaling disrupts zebrafish biliary development and generates multi-organ defects compatible with an Alagille syndrome phenocopy. *Development.* 2004;131:5753-5766.
29. Campbell WA, Yang H, Zetterberg H, Baulac S, Sears JA, Liu T, Wong ST, Zhong TP, Xia W. Zebrafish lacking Alzheimer presenilin enhancer 2 (Pen-2) demonstrate excessive p53-dependent apoptosis and neuronal loss. *J Neurochem.* 2006;96:1423-1440.
30. Ny A, Koch M, Schneider M, Neven E, Tong RT, Maity S, Fischer C, Plaisance S, Lambrechts D, Heligon C, Terclavers S, Ciesiolka M, Kalin R, Man WY, Senn I, Wyns S, Lupu F, Brandli A, Vleminckx K, Collen D, Dewerchin M, Conway EM, Moons L, Jain RK, Carmeliet P. A genetic Xenopus laevis tadpole model to study lymphangiogenesis. *Nat Med.* 2005;11:998-1004.

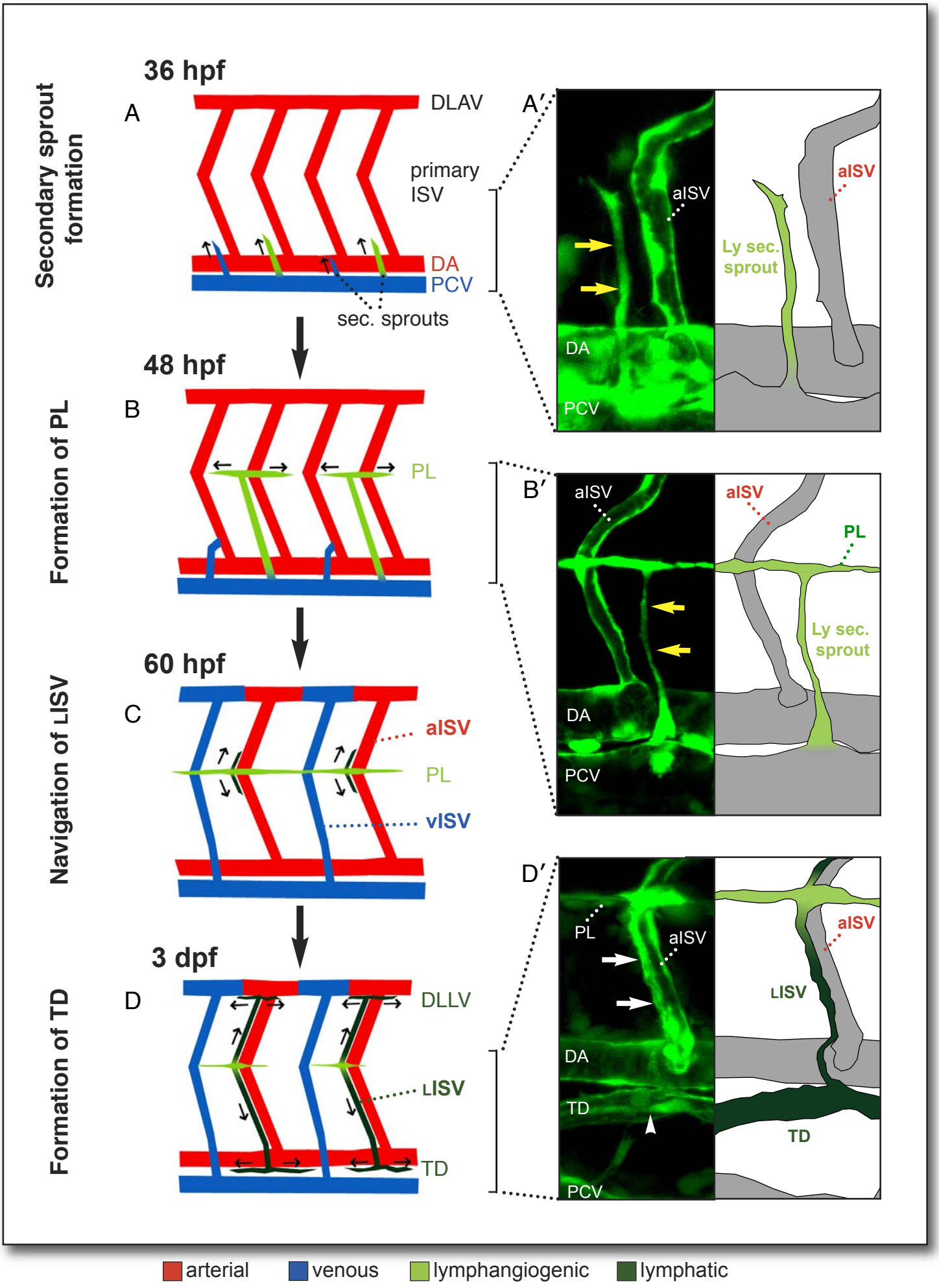

Supplemental Figure I

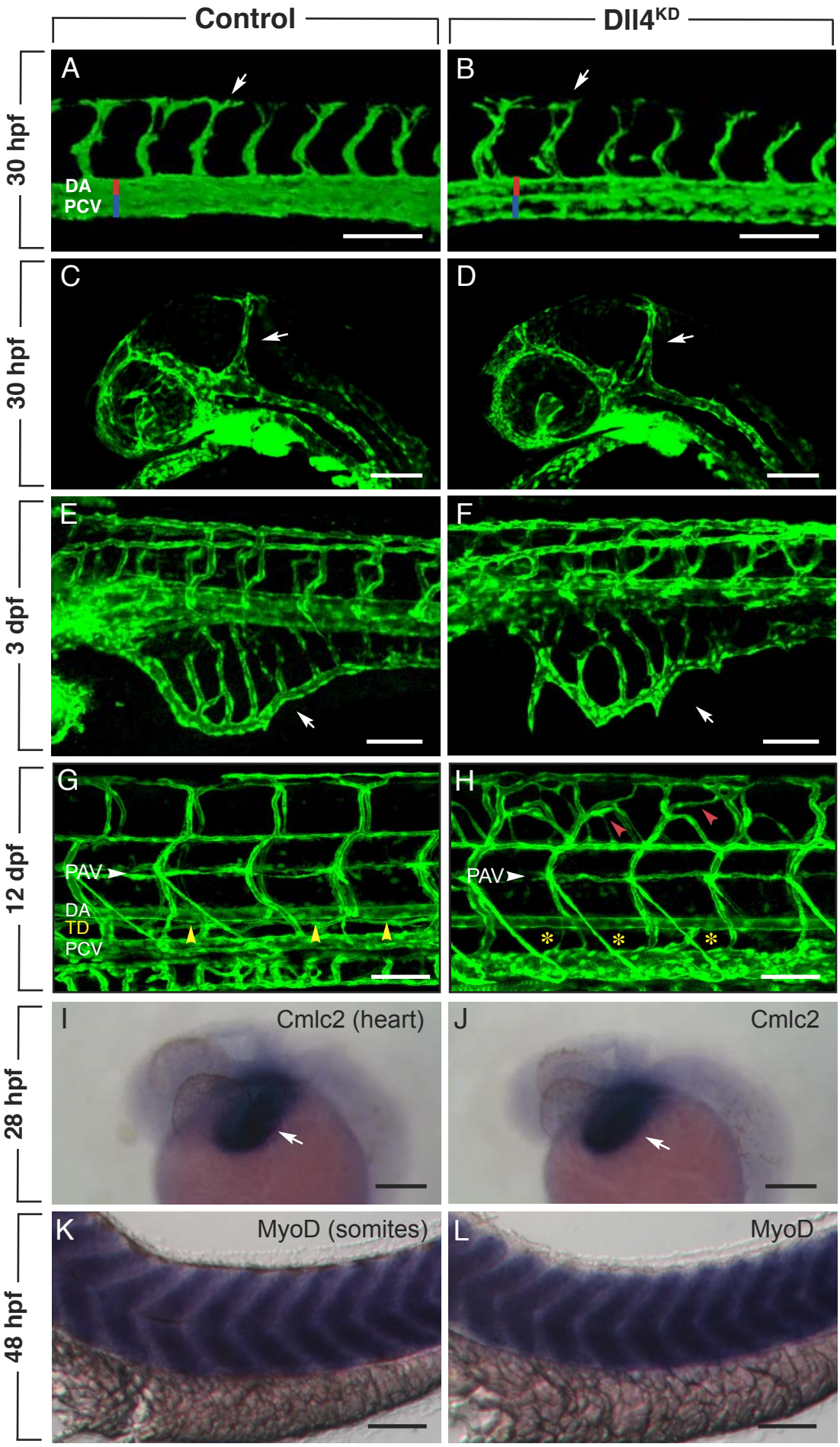

Supplemental Figure II

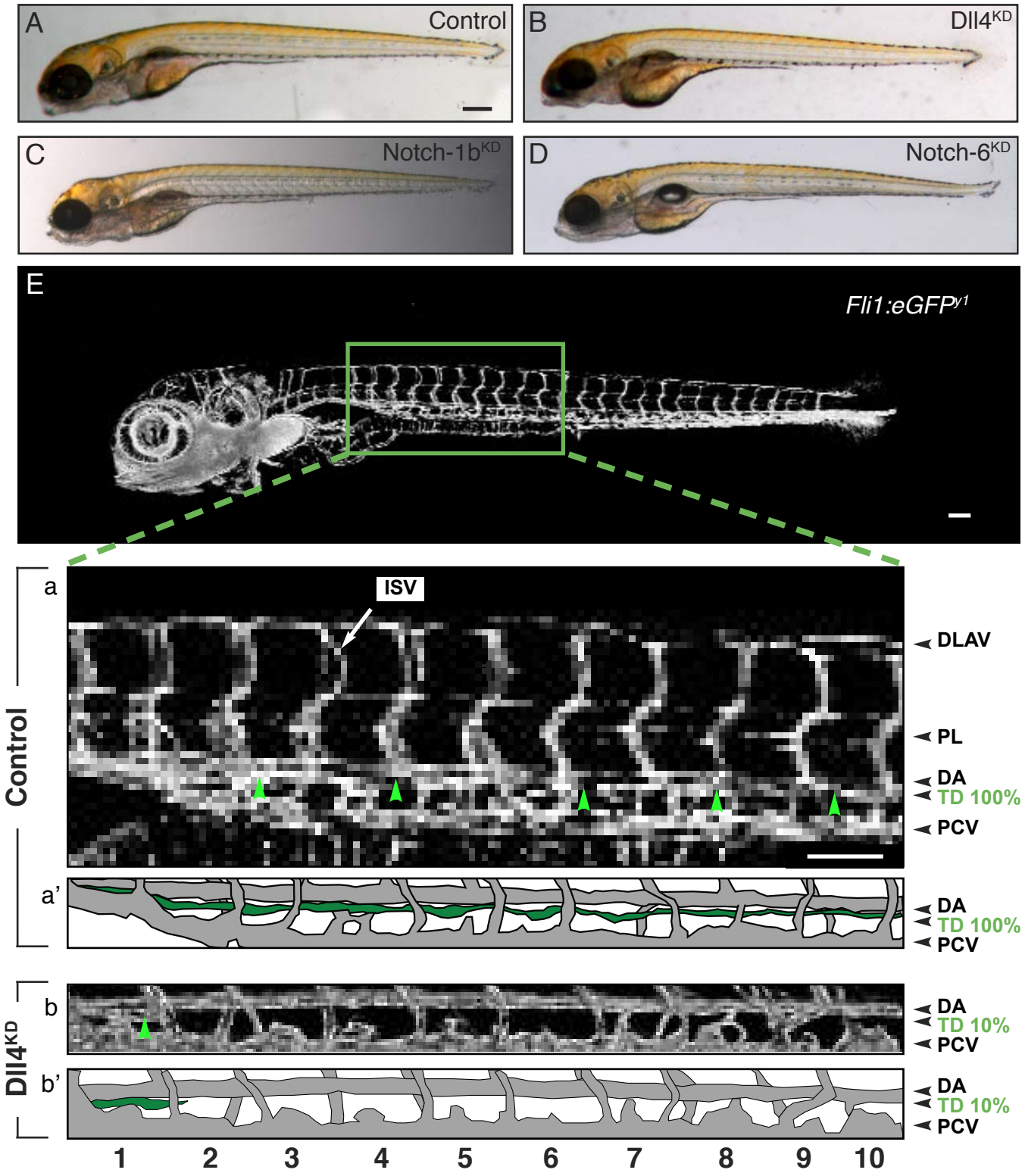

Supplemental Figure III

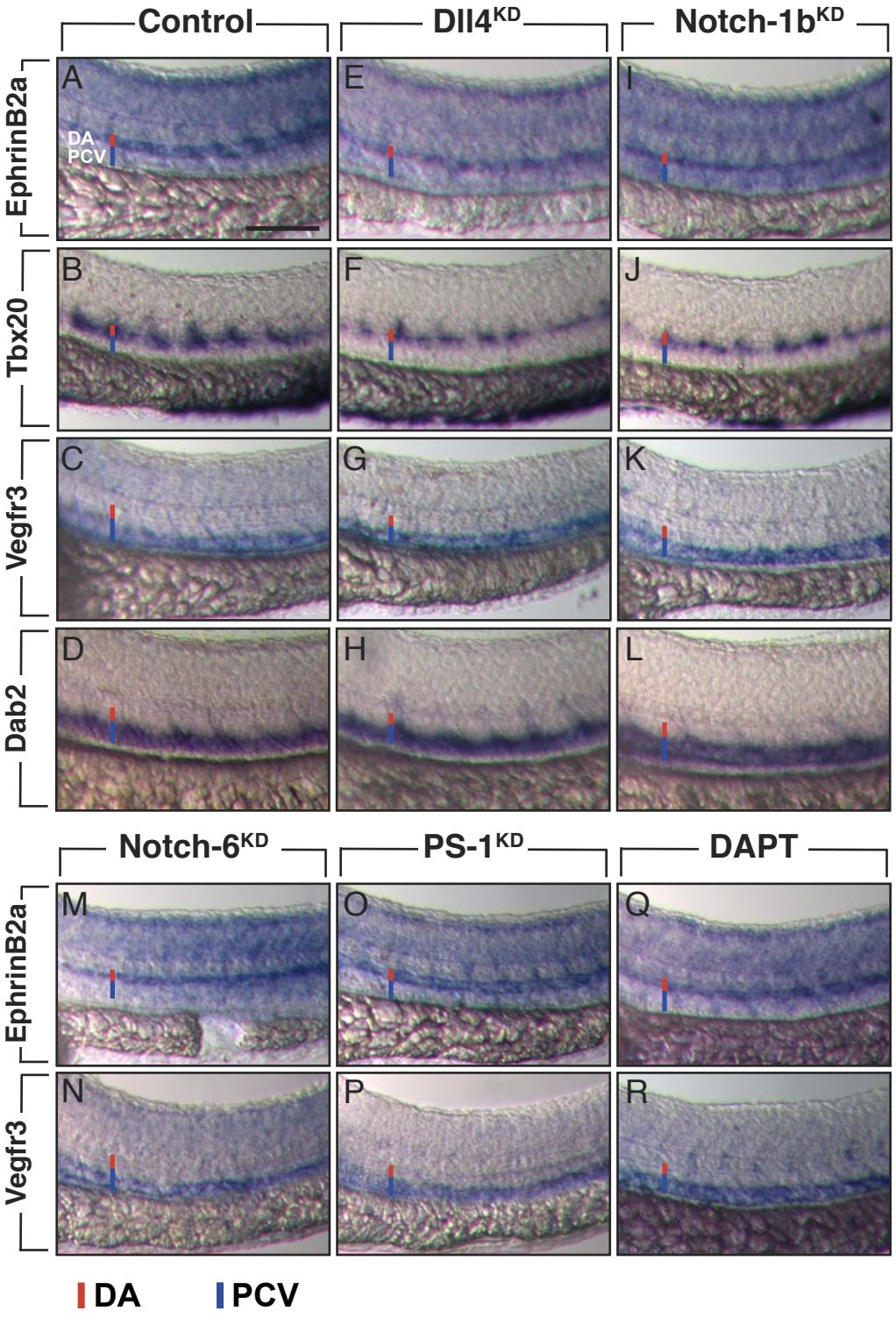

Supplemental Figure IV

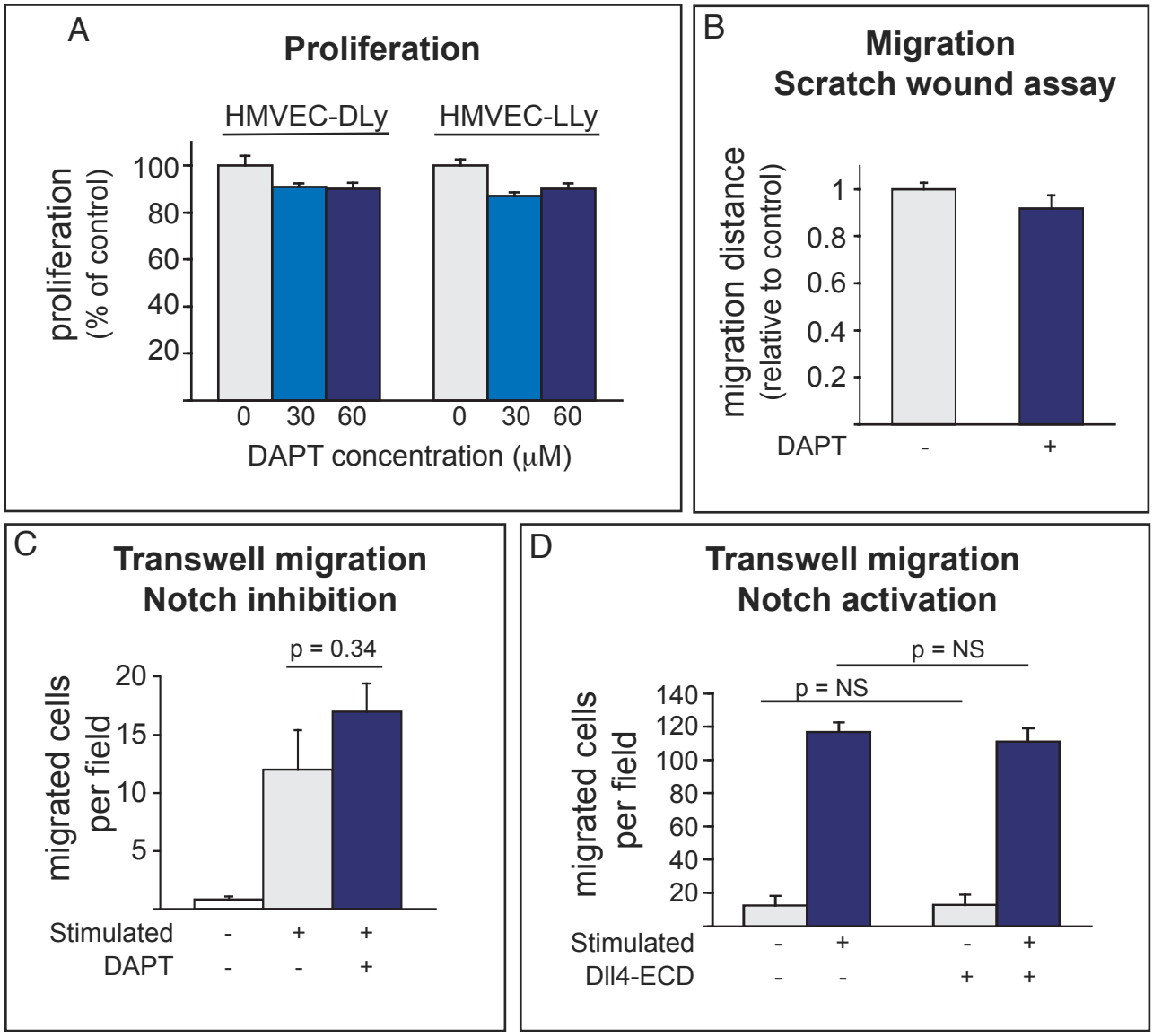

Supplemental Figure V

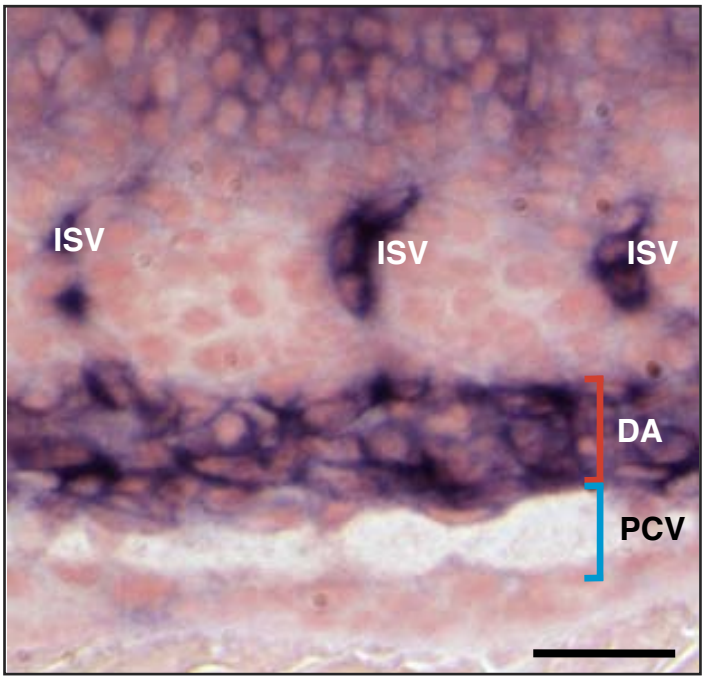

Supplemental Figure VI